Wind bursts and enhanced evaporation in the tropical and subtropical Atlantic Ocean

Kristina B. Katsaros,[a] Alberto M. Mestas-Nuñez,[b]* Abderrahim Bentamy,[c] and Evan B. Forde[a]

[a]National Oceanic and Atmospheric Administration, Atlantic Oceanographic and Meteorological Laboratory, 4301 Rickenbacker Causeway, Miami, Florida 33149, U.S.A.

[b]Cooperative Institute for Marine and Atmospheric Studies, University of Miami, 4600 Rickenbacker Causeway, Miami, Florida 33149, U.S.A.

[c]Institut Français pour la Recherche et l'Exploitation de la MER, BP 70, 29280 Plouzané, France

Satellite-derived estimates of weekly latent heat flux for the tropical and subtropical Atlantic Ocean (40°S to 40°N) were calculated for a one-year period from September 30, 1996 to September 28, 1997 (52 weeks). The oceanic variables required to estimate evaporation (sea surface temperature, surface wind speed, and surface air humidity) were obtained from sensors on several polar-orbiting satellites including the European Remote Sensing satellite 2 (ERS-2), the NASA scatterometer (NSCAT), and the Special Sensor Microwave/Imager (SSM/I). During this period, high values of the weekly satellite estimates of wind speed and latent heat flux were found over the northeast and southeast trade wind regions. In these regions, the 52-week average fields showed wind speeds greater than about 7 m s^{-1} and associated evaporation rates greater than 120 W m^{-2}. The annual cycle dominates the temporal evolution of sea surface temperature but is hardly noticeable in wind speed and latent heat flux, which are dominated by large 3-4 week fluctuations. The most significant event during our period of study was a strong northeast trade wind burst that originated near the northwest African coast in early February 1997. It persisted for five weeks as it crossed the North Atlantic Ocean and finally dissipated in the Caribbean Sea in early March 1997. In the southeast trade region, a similar but less intense period of higher flux was observed during July 1997. These large-scale wind bursts illustrate the strong role that the Atlantic trade winds play in enhancing evaporation.

* Corresponding Author. Email: alberto.mestas@noaa.gov.

1. INTRODUCTION AND BACKGROUND

The interhemispheric water exchange in the ocean is carried out by the meridional overturning circulation, with new deep water being constantly formed in the North Atlantic and around Antarctica and old water returning at the surface [*Toggweiler*, 1994]. The driving mechanism for this circulation is thought to be a combination of buoyancy, involving both heat and fresh water fluxes, and wind forcing [*Csanady*, 2001]. In the tropical Atlantic, the proposed surface return path for the overturning circulation is mostly along the western boundary, where the details of this path involve a complicated surface circulation [*Gordon*, 1986]. Although the wind appears to be the dominant forcing for the return flow in the tropical Atlantic, air-sea buoyancy fluxes also play an important role by continuously modifying the surface water properties.

The main contributor to the air-sea buoyancy fluxes is evaporation, leading to changes in temperature and salinity of the surface waters. The sea surface temperature (SST) variability is due to the large amounts of energy exchanged as latent heat, while the upper ocean salinity changes are due to the net air-sea fresh water fluxes (evaporation minus precipitation). In the atmosphere, the amount of water vapor and its vertical movement throughout the troposphere are directly related to cloud formation, precipitation, and the attendant release of latent heat. Water vapor in the atmosphere is also transported horizontally (*e.g.,* from tropics to poles or from oceans to continents) constituting the atmospheric branch of the global hydrological cycle [*e.g., Peixoto and Oort*, 1992].

Another important role of evaporation is to provide a positive thermodynamic feedback mechanism for air-sea interactions in the tropics [*Xie and Philander*, 1994]. In the tropical Atlantic, this mechanism has been hypothesized to explain decadal changes of the inter-hemispheric SST gradient [*Carton et al*., 1996; *Chang et al*., 1997], which modulates precipitation over northeast South America [*Moura and Shukla*, 1981] and northwest Africa [*Folland et al*., 1986]. Confirming or rejecting this hypothesis is challenging because the heat flux anomalies involved in these tropical air-sea interactions are well below the observational limit of 10-20 W m^{-2} [*Carton et al*., 1996]. Therefore, thorough tests of the role of evaporation in climate await improved estimates of the relevant variables.

In situ and remote observations of the oceanic and atmospheric variables involved in the surface flux calculations are commonly assimilated into numerical atmospheric models. Regions of sparse observations are, as a consequence, also poorly represented in the resulting atmospheric analyses. The sampling problem can only be improved by assimilating more accurate satellite observations. Therefore, it is necessary to keep improving the quality of remotely sensed fluxes. With this in mind, we have chosen to examine current satellite data as a source for the relevant variables involved in the surface latent heat fluxes.

Our methods for estimating global latent heat fluxes and an assessment of the quality of our estimates were presented in *Bentamy et al.* [2003]. Briefly, we follow previous developments for estimating evaporation and latent heat flux by using the ideas originally proposed by *Liu* [1984]. The turbulent latent heat flux,

H_L, was calculated from mean near surface variables using the bulk aerodynamic method:

$$H_L = -l\,\rho\,C_E\,\overline{U}_{10_N}\,(q_{10_N} - q_s), \tag{1}$$

where l is the coefficient for latent heat of evaporation; ρ is the air density; C_E is the bulk transfer coefficient for water vapor [*Smith*, 1988; *Hasse and Smith*, 1997]; $\overline{U}_{10_N}$ is the surface wind speed at 10-m height and neutral stratification; q_{10_N} is the specific humidity at 10-m height and neutral stratification; and q_s is the specific humidity at the sea surface equivalent to the saturation value of SST. The input variables, $\overline{U}_{10_N}$, q_{10_N}, and SST were estimated from satellite observations.

The *Bentamy et al.* [2003] study concentrated on the period October 1996 through June 1997 when several wind sensors on polar-orbiting satellites provided good sampling over the global ocean. During this time period, the NSCAT instrument provided two 500-km swaths per day of data that yielded 25-km resolution wind vectors. Simultaneously, the ERS-2 satellite obtained a single 500-km swath of wind vectors at 50-km resolution, while several microwave radiometers in the Defense Meteorological Satellite Program (DMSP) provided wind speeds over 1400-km swaths at 50-km resolution. These SSM/Is provided near surface humidity by a proxy estimate [*Schulz et al.,* 1993, 1997]. The other variable needed, SST, was obtained from the Reynolds analysis [*Reynolds and Smith*, 1994]. The resulting weekly and monthly global evaporation rate estimates were produced at the Institut Français pour la Recherche et l'Exploitation de la Mer (IFREMER) in France. These estimates compared well with the Comprehensive Ocean-Atmosphere Data Set (COADS) data and with surface flux estimates produced by numerical analyses at the National Centers for Environmental Prediction/National Center for Atmospheric Research (NCEP/NCAR) and the European Center for Medium-Range Weather Forecasts (ECMWF). Details of these comparisons are shown in *Bentamy et al.* [2003], where differences between satellite estimates and numerical analyses estimates are discussed.

In the present study, we focus on the subtropical and tropical Atlantic Ocean (40°S to 40°N) for a detailed study of the patterns of SST, surface wind, and latent heat flux for the one-year period September 30, 1996 to September 28, 1997 (52 weeks). We use the 1° × 1° gridded weekly-averaged latent heat flux fields of *Bentamy et al.* [2003] but have extended the calculations to one full year. The reader must note that the lack of NSCAT wind observations beyond June 1997 does not significantly affect our results. We have chosen to include the surface wind speed and not the SST plots in the series of weekly averages that follow. The SST in the tropical ocean varies only a few degrees Celsius during the year, while the surface wind speed is more dynamic and varies by a factor of 5 to 10, even in the weekly average, and is the dominant variable in latent heat flux variability.

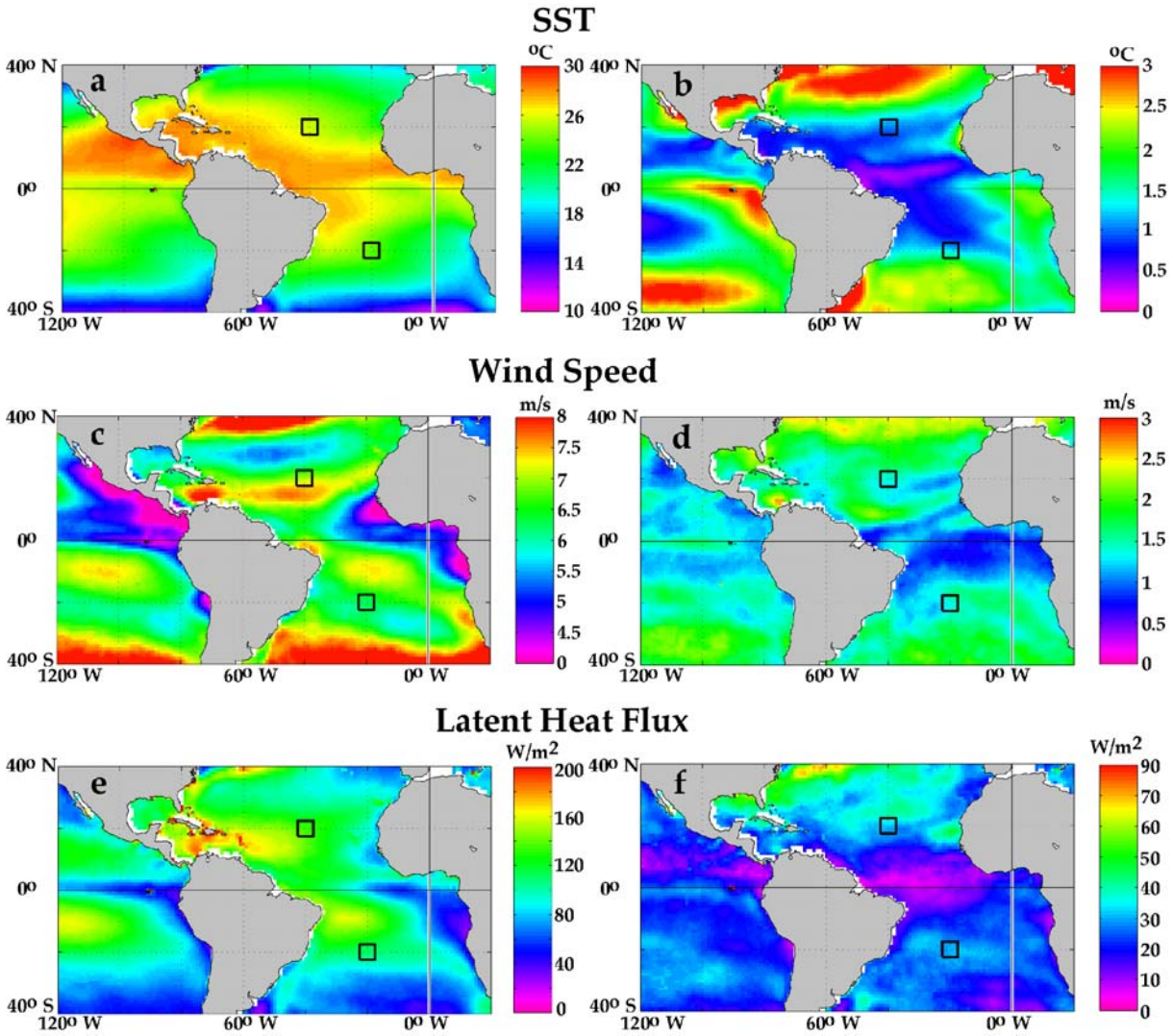

Figure 1. Respective mean and standard deviation maps of weekly-averaged fields of sea surface temperature (SST) in °C (a, b), wind speed in m s^{-1} (c, d), and latent heat flux in W m^{-2} (e, f) for September 30, 1996-September 28, 1997. The squares denote areas used for calculating the time series in Figure 2.

2. RESULTS

2.1. Mean Values and Standard Deviations

The patterns of the mean and standard deviations of the satellite-derived variables for SST, wind speed, and latent heat flux are examined (Figure 1). The mean fields have structure similar to that of annual climatological estimates [*e.g., Esbensen and Kushnir*, 1981].

The mean SST (Figure 1a) is dominated by the western hemisphere warm pool (SST >28.5°C) [*Wang and Enfield*, 2001] which surrounds the tropical American continent and extends eastward along the thermal equator, a region known as the Inter-Tropical Convergence Zone (ITCZ). From the standard deviation map (Figure 1b), the SST variation is generally small in the tropical Atlantic.

Exceptions are regions of moderate variability (annual standard deviations of the weekly average between 1.5 and 2.5°C) in the seasonal upwelling regime off northwest Africa and in the eastern Atlantic equatorial cold tongue, and a region of larger variability (standard deviations larger than 2.5°C) in the Gulf of Mexico. Note the weaker variability of the cold tongue in the eastern tropical Atlantic (standard deviations everywhere <2.5°C) compared to the equatorial cold tongue in the eastern tropical Pacific (standard deviations can be >3°C).

The mean wind speed (Figure 1c), which is based on the 10-m neutral stratification estimate of the total wind vector, is dominated by the trade winds in the tropics and the westerly winds at higher latitudes. The standard deviation of weekly-averaged wind speeds (Figure 1d) has larger values in the northern than in the southern tropical Atlantic, with maximum values higher than 3 m s^{-1} in the Caribbean Sea. In the extratropics, the regions of large weekly variability are associated with the band of the westerlies poleward of 30° latitude.

The mean latent heat flux (Figure 1e) has large values (>120 W m^{-2}) in the trade wind regions in both the Atlantic and Pacific with the patterns relative to the equatorial cold tongue looking quite similar. In the Atlantic, the maximum latent heat fluxes are in the Caribbean and western Atlantic Ocean at 10-20°N and off Brazil at 5-15°S, from about 20°W to the Brazilian coast. There are weak values of evaporation off northwest Africa associated with weaker winds near the mean location of the ITCZ (see Figure 1c). Weak latent heat fluxes (<50 W m^{-2}) are also found in the cold tongue region of the eastern tropical Atlantic associated with the cooler waters there (see Figure 1a). The standard deviation of latent heat flux (Figure 1f) shows values smaller than 30 W m^{-2} over most of the tropical Atlantic and larger than 40 W m^{-2} in the Caribbean, Gulf of Mexico, middle and higher latitudes in the North Atlantic, and the eastern and western subtropical South Atlantic. There are low values of the standard deviation in the central subtropical South Atlantic near the Greenwich meridian associated with the northward extent of cooler high-latitude surface waters (see Figure 1a).

In Figure 2, the temporal evolution of SST, wind speed, and latent heat flux at two selected (North and South Atlantic) locations indicated by black boxes in Figure 1 are illustrated. The locations are subjectively selected near the warmer waters of the Atlantic warm pool (Figure 1a) and on the poleward side of the easterly wind bands (Figure 1c). In these regions, the mean latent heat fluxes (Figure 1e) have moderate values (about 120 W m^{-2}) and the standard deviations (Figure 1f) have typical maximum values (about 40-50 W m^{-2}) for the interior tropical-subtropical Atlantic. The SST evolution (Figure 2, upper panel) clearly shows the seasonal warming and cooling (180° out of phase) in both hemispheres [*e.g., Carton and Zhou*, 1997). There is little or no evidence, however, for the seasonal cycle in wind speed (Figure 2, middle panel) and latent heat flux (Figure 2, bottom panel). Both wind speed and latent heat flux are dominated by 3-4 week fluctuations with respective typical ranges of about 3 m s^{-1} and 50 W m^{-2}. Sometimes the changes can be twice as large, such as in the northern hemisphere during February 1997, due to a strong easterly wind burst described below.

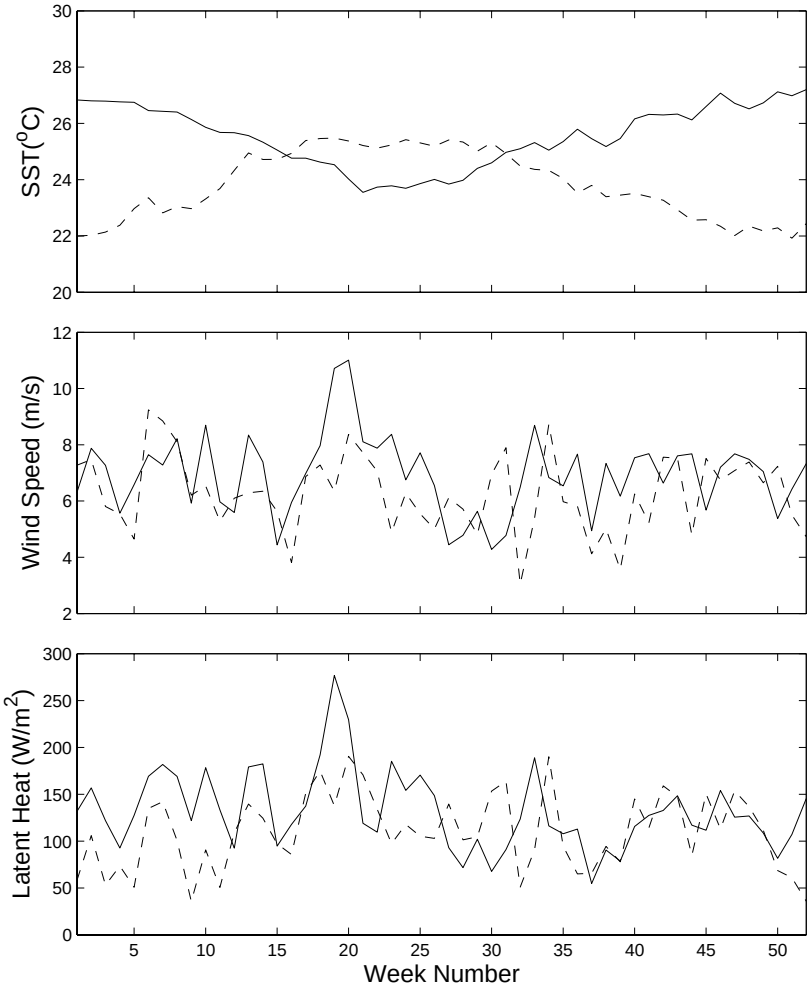

Figure 2. Time series of weekly SST (upper panel), surface wind speed (middle panel), and latent heat flux (lower panel) averaged in two areas (17-22.5°N, 37.5-42.5°W; 22.5-17.5°S, 17.5-22.5°W) representing the northeasterly (solid line) and southeasterly (dashed line) trade wind regions, respectively. The locations of these areas are indicated with squares in Figure 1. The week number starts with the week of September 30-October 6, 1996 and ends with the week of September 22-28, 1997.

2.2. Wind Bursts and Associated Latent Heat Flux

Four periods are chosen to show patterns of enhanced latent heat flux due to wind bursts that take several weeks to subside or to cross the Atlantic Ocean.

(1) **November 4-24, 1996**. During this three-week period, the trade winds in both the North and South Atlantic reach mean weekly-averaged wind speeds greater than 8-10 m s^{-1}, with associated weekly-averaged latent heat flux greater than about 200 W m^{-2} (Figure 3). Although the wind speeds have similar magnitude in both hemispheres, the latent heat fluxes of the northeast trades are larger because of the warmer waters of the eastern tropical Atlantic. In Figure 3, regions of large wind speed generally correspond with regions of large latent heat flux, illustrating the visual coherence between the wind and latent heat flux patterns.

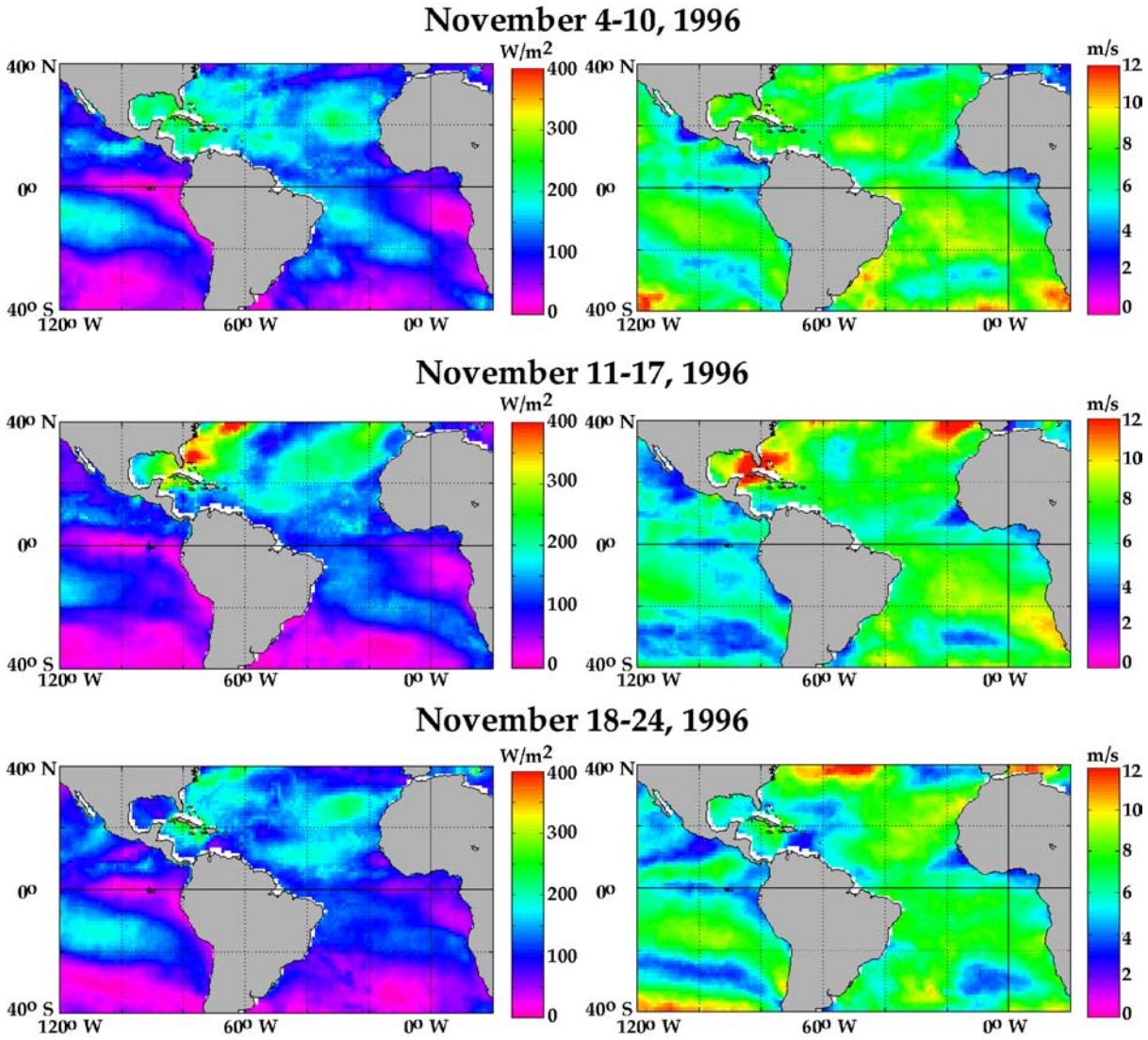

Figure 3. Weekly-averaged latent heat flux (left panels) and wind speed (right panels) for a sequence of three weeks in November 1996 illustrating the correlation between surface wind speed and latent heat flux.

(2) **February 3-March 9, 1997.** During this five-week period in the Northern Hemisphere winter, a large area of high wind speed (>12 m s^{-1}) in the northeast trade wind region persists across the Atlantic Ocean from 30°N, 20°W to the northern Brazilian coast, which gradually translates into the Caribbean Sea (Figure 4). It continues to penetrate into the Caribbean over this five-week period, gradually subsiding to wind speeds of about 8 m s^{-1} in the eastern Atlantic. The area covered by these higher winds also diminishes to about one-quarter of its original size during the translation. The associated latent heat flux values are at a maximum of about 325 W m^{-2} during the first weeks, gradually decreasing to 150-200 W m^{-2} during the last two weeks of this period, with very low values persisting throughout (<100 W m^{-2}) in a wedge along the Moroccan coast. This type of enhanced ocean forcing cannot be readily seen in other surface flux data sets.

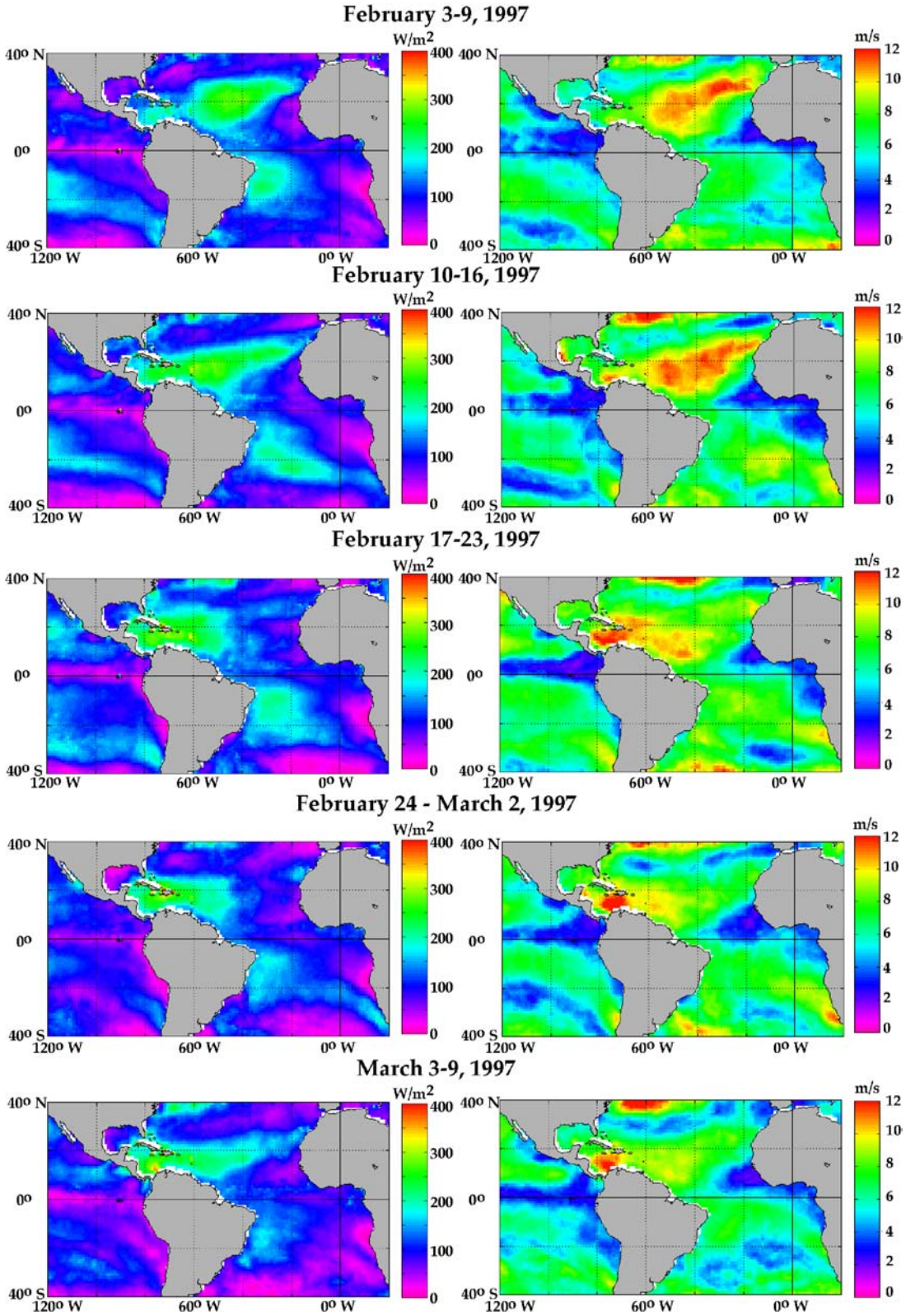

Figure 4. Weekly-averaged latent heat flux (left panels) and wind speed (right panels) for a five-week period in February-March 1997. A widespread wind burst in the northeast trades is seen to translate into the Caribbean.

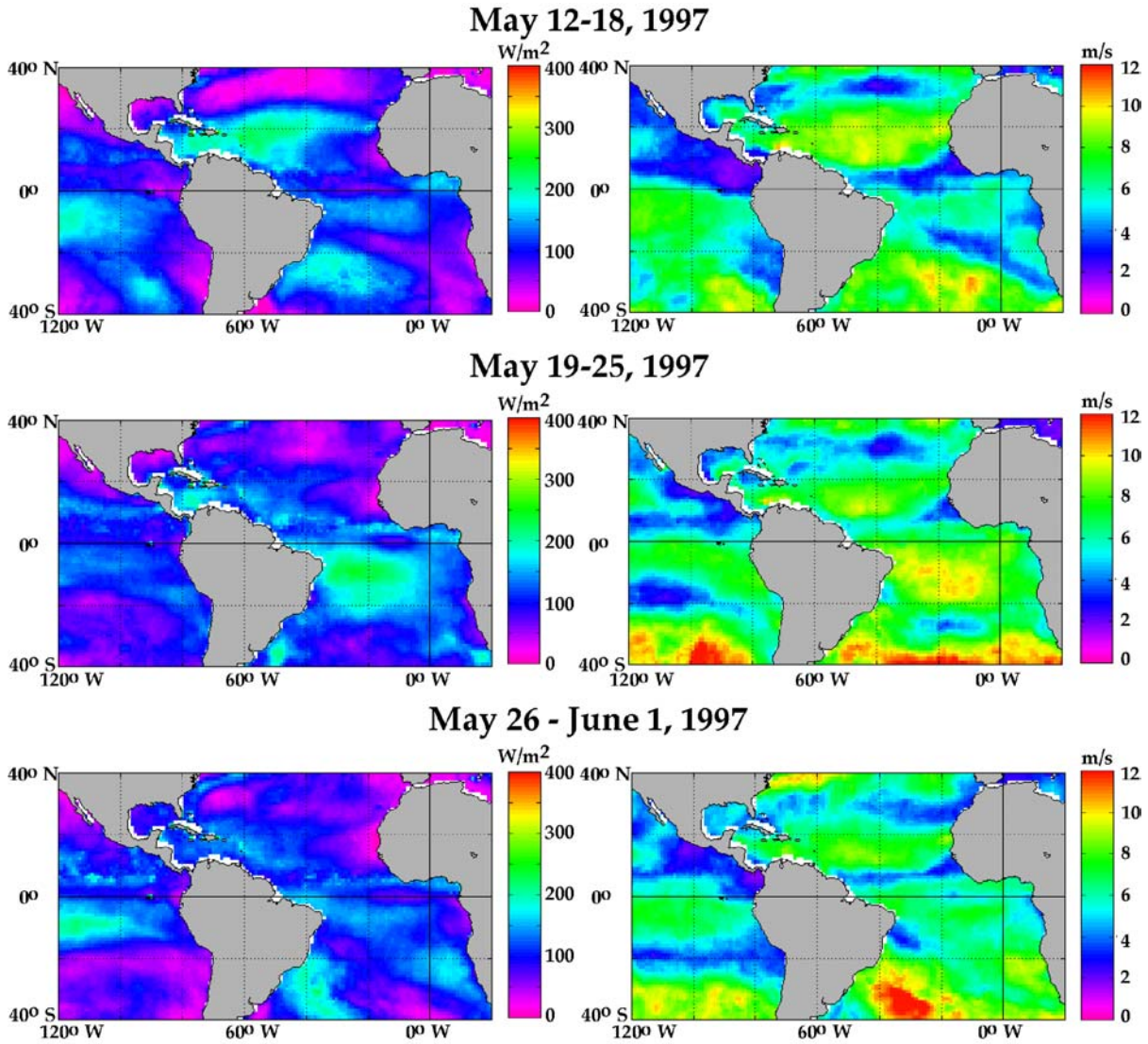

Figure 5. Weekly-averaged latent heat flux (left panels) and wind speed (right panels) for a three-week period in May-June 1997.

(3) **May 12-June 1, 1997.** This three-week period includes weekly averages with strongest winds in the southeast trade wind region of the Atlantic Ocean (Figure 5). The pattern is not as dramatic, widespread, or persistent as the one in the northeast trades in November 1996. The correlation between wind speed and evaporation rate is very clear in these images with the exception of the region off northwest Africa. The same wind speeds as in the central North Atlantic at 10-20°N give less than half the latent heat fluxes over the cool waters off the African coast. Thus, the correlation of evaporation rate with wind speed cannot be taken as a given. During this three-week period there is a strengthening of the southeast trades in the second week and a weakening in the third week.

(4) **June 30-July 20, 1997.** At the height of the southern hemisphere winter, we also see a period of enhanced wind speeds in the southeast trades (Figure 6).

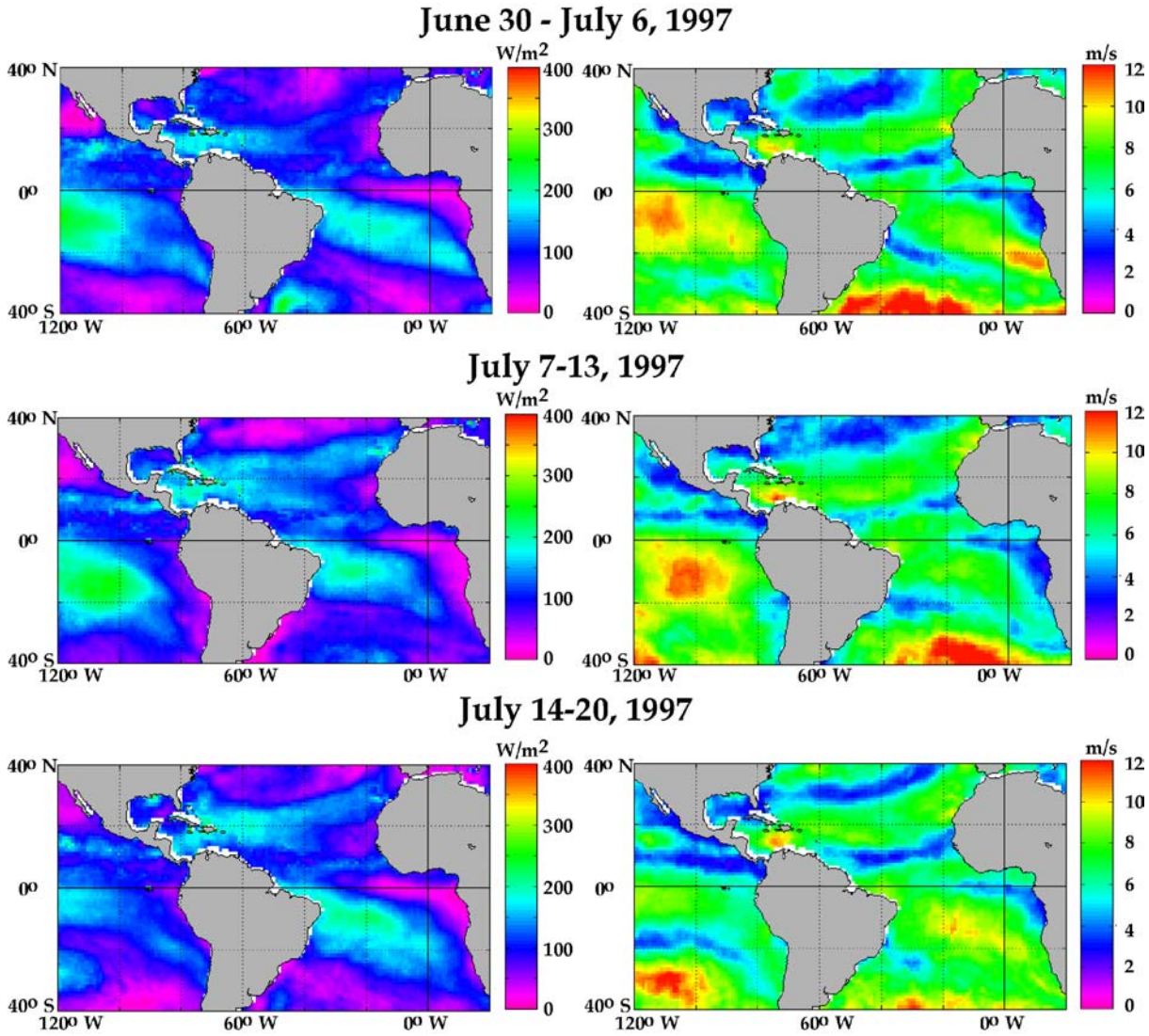

Figure 6. Weekly-averaged latent heat flux (left panels) and mean wind speed (right panels) for a three-week period in June-July 1997.

No apparent westward propagation, as was illustrated for the period February-March 1997 in the northern hemisphere winter, is seen in this case. However, a large region south of 2°S streaking towards the northwest has increased wind speeds and latent heat fluxes. The southeast trades and their latent heat fluxes abate in the intermediate week of July 7-13, 1997, similar (and opposite) to that observed during May-June 1997. This large-scale strengthening and weakening of the trades in alternating weeks appears to be a common occurrence in both hemispheres during the study period (see also Figure 2).

3. CONCLUDING REMARKS

We have presented and described weekly fields of SST, wind speed, and latent heat flux in the tropical and subtropical Atlantic for a one-year period (October

1996 to September 1997). Our main result is the observance of strong 3-4 week fluctuations in wind speed and latent heat fluxes during our study period. Large-scale increases and decreases with ranges of about 3 m s^{-1} and 50 W m^{-2} are typical in the trade wind regions of both hemispheres but are more noticeable in the northern hemisphere. Occasionally, these wind bursts may be twice as strong, last for several weeks, and translate westward across the Atlantic Ocean (such as during February 1997), having a pronounced effect on evaporation rates.

Earlier work on oceanic circulation has depended on monthly, seasonally, or climatologically averaged winds. With the launch of the ERS-1 satellite in 1991, 10-day averaged wind fields could be generated and used to force models of the tropical Atlantic Ocean [*e.g., Bentamy et al.,* 1996]. Numerical atmospheric models, in particular, the NCEP/NCAR reanalyses, are presently used in many atmosphere-ocean studies. However, the verification of NCEP/NCAR model flux statistics could not be obtained without data sets such as the one in this study.

The present data set is not currently adequate as input for ocean circulation models since it does not provide all the terms in the heat and mass budget. The terms for short and longwave radiative fluxes, downward and upward directed, and the sensible heat flux must also be taken into account in the total heat budget, and precipitation is also needed to calculate the mass budget. The temporal and spatial relationships between maximum solar heating (outside the ITCZ), the maximum evaporation rate, and maximum momentum flux may have interesting mesoscale effects in the ocean. Plans are underway to complete the Atlantic heat budget for the one-year period (October 1996-September 1997) reported in this paper and to extend the record to cover the 10-year period from 1991-2001.

Acknowledgments

Financial support for this work has been provided by NASA grant NRA 99 OES-10, an IFREMER grant in support of Alberto Mestas-Nuñez, and by NOAA internal support to Kristina Katsaros for using microwave sensors in oceanographic research. The NSCAT data came from the Physical Oceanography Distributed Active Archive Center (PODAAC), the ERS data from the European Space Agency and Centre de ERS d'Archivage et de Traitment (CERSAT), and the SSM/I data from the EOS Distributed Archive Center at Marshall Space Flight Center, Alabama. An animation of the weekly latent heat flux fields is available online (www.aoml.noaa.gov/rsd/satellite/lhfyrmov.gif) or on a CD-ROM by writing to Mr. Evan Forde. We appreciate the work of Ms. Gail Derr in manuscript production.

REFERENCES

Bentamy, A., Y. Quilfen, F. Gohin, N. Grima, M. Lenaour, and J. Servain, Determination and validation of average wind fields from ERS-1 scatterometer measurements, *Global Atmos. Ocean Sys., 4* (1), 1-29, 1996.

Bentamy, A., K.B. Katsaros, A.M. Mestas-Nuñez, W.M. Drennan, E.B. Forde, and H. Roquet, Satellite estimates of wind speed and latent heat flux over the global oceans, *J. Climate, 16* (4), 637-656, 2003.

Carton, J.A., X. Cao, B.S. Giese, and A.M. da Silva, Decadal and interannual SST variability in the tropical Atlantic Ocean, *J. Phys. Oceanogr.*, *26* (7), 1165-1175, 1996.

Carton, J.A., and Z. Zhou, Annual cycle of sea surface temperature in the tropical Atlantic Ocean, *J. Geophys. Res., 102* (C13), 27,813-27,824, 1997.

Chang, P., L. Ji, and H. Li, A decadal climate variation in the tropical Atlantic Ocean from thermodynamic air-sea interactions, *Nature*, *385* (6616), 516-518, 1997.

Csanady, G.T., *Air-sea Interaction: Laws and Mechanisms,* Cambridge University Press, New York, 239 pp., 2001.

Esbensen, S.K., and Y. Kushnir, The heat budget of the global ocean: An atlas based on estimates from surface marine observations, Climate Research Institute, Rep. 29, Oregon State University, 27 pp. and 188 figs, 1981.

Folland, C.K., T.N. Palmer, and D.E. Parker, Sahel rainfall and worldwide sea temperatures, *Nature*, *320* (6063), 602-607, 1986.

Gordon, A.L., Interocean exchange of thermocline water, *J. Geophys. Res., 91* (C4), 5037-5046, 1986.

Hasse, L., and S.D. Smith, Local sea surface wind, wind stress, and sensible and latent heat fluxes, *J. Climate, 10* (11), 2711-2724, 1997.

Liu, W.T., Estimation of latent heat flux with Seasat-SMMR: A case study in the North Atlantic, in *Large-Scale Oceanographic Experiments and Satellites,* edited by C. Gautier and M. Mieux, pp. 205-221, D. Reidel Publishing, Dordrect, 1984.

Moura, A.D., and J. Shukla, On the dynamics of droughts in northeast Brazil: Observations, theory, and numerical experiments with a general circulation model, *J. Atmos. Sci.*, *38* (12), 2653-2675, 1981.

Peixoto, J.P., and A.H. Oort, *Physics of Climate,* American Institute of Physics, New York, 520 pp., 1992.

Reynolds, R.W., and T.M. Smith, Improved global sea surface temperature analyses using optimum interpolation, *J. Climate, 7* (6), 929-948, 1994.

Schulz, J., P. Schlüssel, and H. Grassl, Water vapor in the atmospheric boundary layer over oceans from SSM/I measurements, *Int. J. Remote Sens., 14* (15), 2773-2789, 1993.

Schulz, J., J. Meywerk, S. Ewald, and P. Schlüssel, Evaluation of satellite-derived latent heat fluxes, *J. Climate, 10* (11), 2782-2795, 1997.

Smith, S.D., Coefficients for sea surface wind stress, heat flux, and wind profiles as a function of wind speed and temperature, *J. Geophys. Res., 93* (C12), 15,467-15,472, 1988.

Toggweiler, J.R., The ocean's overturning circulation, *Physics Today, 47* (11), 45-50, 1994.

Wang, C., and D.B. Enfield, The tropical western hemisphere warm pool, *Geophys. Res. Lett., 28* (8), 1635-1638, 2001.

Xie, S.P., and S.G.H. Philander, A coupled ocean-atmosphere model of relevance to the ITCZ in the eastern Pacific, *Tellus A*, *46* (4), 340-350, 1994.